15 Aug 2008, 11:00am - 12:30pm

Numerical Analysis of Algonquin Geogrid Reinforced Soil Retaining Wall under Construction and Earthquake Loading

Javad Safadoust
University of Tabriz, Tabriz, Iran

Golam Moradi
University of Tabriz, Tabriz, Iran


6th International Conference on
Case Histories in Geotechnical Engineering, Arlington, VA, August 11-16, 2008

NUMERICAL ANALYSIS OF ALGONQUIN GEOGRID REINFORCED SOIL RETAINING WALL UNDER CONSTRUCTION AND EARTHQUAKE LOADING

Javad Safadoust
University of Tabriz
Tabriz, Iran

Golam Moradi
University of Tabriz
Tabriz, Iran

ABSTRACT

In this paper the finite element procedure was used to investigate the behavior of 6.1m high Algonquin geogrid reinforced soil retaining wall using the computer program Plaxis under construction and earthquake loading. Algonquin wall was constructed in Algonquin, Illinois by FHWA (Federal Highway Administration).The performance of the wall was measured during the construction using inclinometers and surface optical surveys for deflection, and strain gauges for reinforcement strain distribution. In order to investigate the effect of earthquake loading on the wall performance, the 1994 Northridge earthquake motion was applied as input ground motion in the dynamic analysis. The lateral displacement, reinforcement force and vertical stress under earthquake loading were compared to the end of construction. The results show that there is a reasonable agreement between the instrumentation measurement and the finite element analysis for the reinforcement strain distribution and lateral displacement of the wall, and the vertical stress at the just back of the facing panels is less than γz. Also, the largest lateral displacement due to earthquake loading occurs at the top of the wall.

INTRODUCTION

Geosynthetic reinforced soil (GRS) retaining walls have been extensively used in recent years mainly because of their cost benefit, easy construction and flexibility with respect to conventional retaining structures. Another benefit of the GRS retaining walls is the outstanding performance during seismic events. The seismic performance of GRS retaining walls is proven. Worldwide experience in nearly all of the major earthquakes of the last thirty years have provided ample data on the structural stability of mechanically stabilized earth (MSE) structures during seismic loading. The flexibility nature of these walls and their highly absorbing ability are the main cause of their good earthquake performance. The survey conducted by Sandri [1994] indicated that only 2 of 11 MSE structures located within 23-113 km of the Northridge earthquake epicenter of January 17, 1994 showed tension cracks within and behind the reinforced soil mass after the earthquake.

Finite-element analysis is essential for understanding the behavior of GRS walls, particularly prediction of lateral deflection and lateral earth pressure of wall during earthquake loading. Finite element modeling has been frequently used for the static analysis of GRS walls (Rowe and Ho [1992], Karpurapu and Bathurst [1995], and Helwany et al. [1999]). Dynamic finite element modeling for reinforced soil walls is much more limited. Segrestin and Bastick [1988] used the programs SUPEPFLUSH to study the seismic response of reinforced soil walls that used inextensible reinforcement. Bathurst and Hatami [1998] used the dynamic finite-difference program FLAC to perform a parametric analysis of geosynthetic reinforced propped panel walls. Helwany and McCallen [2001] described a finite-element analysis, using DYNA3D, of two 6-m-high segmental retaining walls subjected to horizontal earthquake loading.

This paper describes a plane strain finite element analysis, using PLAXIS, of a 6.1-m-high GRS wall under construction and earthquake loading.

PROJECT BACKGROUND

Algonquin geogrid wall was constructed in a gravel pit in Algonquin, Illinois, a part of a Federal Highway Administration investigation of the behavior of MSE walls (Christopher [1993]). The section of the wall is 6.1m tall and contain 5 segmental concrete panels (three full facing panels and two half panels) with 8 layers of reinforcement. Reinforcements have a constant vertical space of 0.75m and length of 4.3m (Fig. 1). The gravelly sand backfill used was a well graded gravelly sand with a maximum particle size of 50mm and a d_{50} size of 4mm. Foundation condition beneath the wall consisted of 5m of dense gravelly sand underlain by very dense sandy silt. The backfill soil was compacted to 95 percent of standard proctor (ASTM D 698). This was typically obtained with four to five passes of the compactor by using a

lift thickness of approximately 200mm. Bonded strain gauges were attached in pairs at each measurement point.

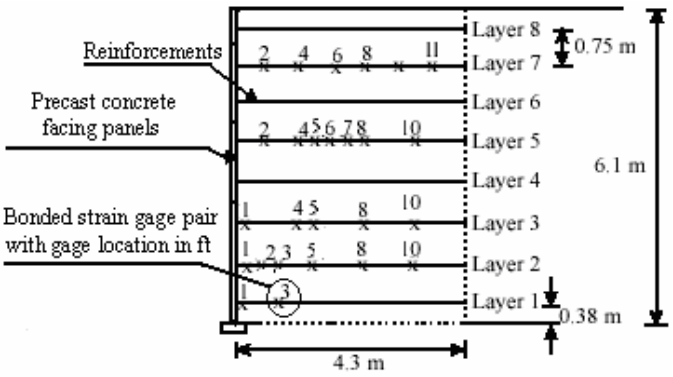

Fig. 1. Wall geometry and instrumentation plan (after Lee et al. [1999]).

SELECTION OF MODEL PARAMETERS

Backfill soil, reinforcement and facing properties are shown in Table 1. The soil modulus is determined using the modified hyperbolic soil modulus model presented by Duncan et al. [1980] during construction as shown in equation 1.

$$E_i = K.P_a.\left(\frac{\sigma_3}{P_a}\right)^n \qquad (1)$$

Where K and n = Primary loading model parameters relating the initial modulus, E_i, to the confining stress, σ_3.
P_a and σ_3 = atmospheric pressure and confining stress, respectively.

Soil/reinforcement interface friction angle is equal to 28.7º.

EARTHQUAKE MOTION

The earthquake motion used in the dynamic analysis is shown in Fig. 2. The 1994 Northridge earthquake, station = Los Angeles, and epicentral distance = 19.2 km, record was considered as input for the base acceleration. The peak acceleration of record is 0.41g.

FINITE ELEMENT MODEL

The wall was modeled as a plane-strain, two dimensional problems for the finite element analysis. Fig. 3 shows the soil mesh used for the analysis. The soil elements are triangular, 15 nodes and Mohr - Coulomb model was used to model soil Behavior. Wall construction was modeled in eight stages, and variation of soil modulus was considered in each stage as equation 1. For this study, reinforcement and the wall facing materials were modeled as linear elastic elements. The reinforcements were modeled using geotextile elements with axial stiffness only, and the facing panels were modeled using beam elements with bending and axial stiffnesses. Interface elements were used to model soil/reinforcement interface.

The absorbent vertical boundaries were generated at the left-hand and the right-hand boundary. An absorbent boundary is aimed to absorb the increment of stresses on the boundaries caused by dynamic loading, that otherwise would be reflected inside the soil body. The earthquake was modeled by means of a prescribe displacement at the bottom boundary.

Table 1. Material Properties of Algonquin Wall: (a) Geogrids (b) Facing panels, (c) Soil.

(a)

Geogrid Properties	Values
Strength	T_{peak}= 67.7 KN/m
Strain	ε_{peak}= 16.0%
Stiffness	$J_{2\%}$ =1020 KN/m

(b)

Facing properties	Values
Modulus of elasticity(MPa)	23950
Moment of inertia (m^4/m)	3.7×10^{-4}
Area (m^2/m)	0.165

(c)

Soil Properties	Values
Friction angle	43 deg
Dilation angle	15 deg
Cohesion	0 deg
Unit weight (KN/m^3)	20.4
Hyperbolic model parameters	K=1100 n=0.5

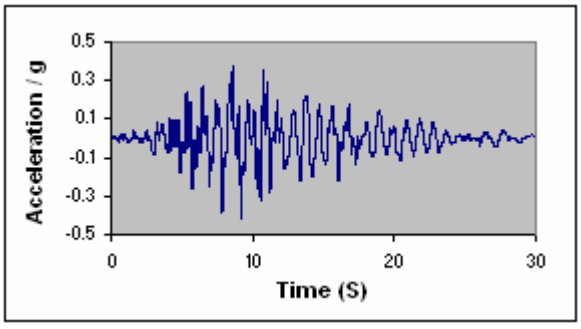

Fig. 2. Acceleration history of 1994 Northridge earthquake

WALL PERFORMANCE DURING CONSTRUCTION

The lateral deflection of the wall and the reinforcements strain distribution of wall are investigated and compared with the instrumentation measurements. Internal vertical stress within the reinforcement mass is compared with γz values.

Lateral Deflection of Wall

The lateral deflection of the wall is shown in Fig. 4. It is seen that model of geogrid wall predicts the lateral deflection of wall within reasonable agreement in comparison to the survey values. The maximum deflection of wall is about 0.5% of the wall height.

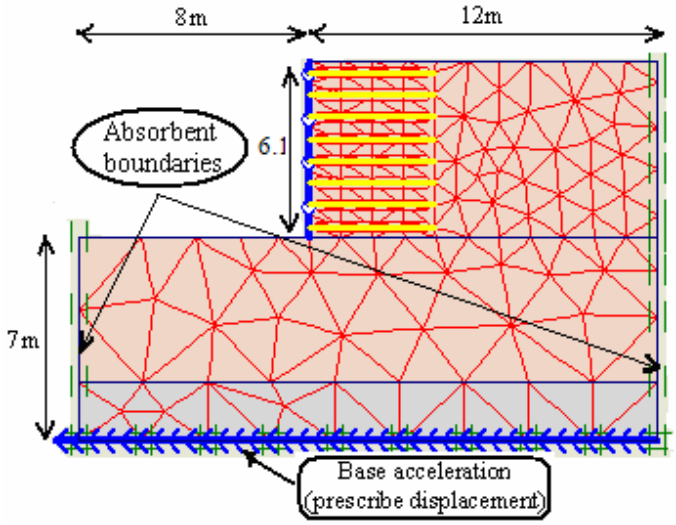

Fig. 3. FEM mesh for the Algonquin wall.

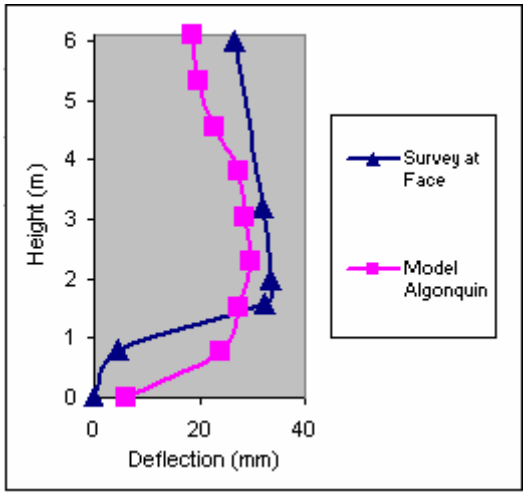

Fig. 4. Face deflection of Algonquin wall at the end of construction.

Reinforcements Strain Distribution

As shown in Fig. 5, the results of the model show good agreement with instrumentation measurements of layers 2 and 5, for both maximum strain magnitudes and locations at the end of construction. Model Algonquin tended to over-estimate the reinforcement strains at layer 1. For layers 3 and 7, as shown in fig. 5, model Algonquin gave reasonable predictions of magnitudes and locations of the maximum reinforcement strains at the end of construction.

Instrumentation and modeling results indicated that the reinforcement strain increased from top of the wall as depth increased, and reach their maximum value at elevations between 0.35H to 0.15H, where H is the height of wall. After reaching their maximum values, the reinforcement strains started to decrease and had small values at the bottom of the wall.

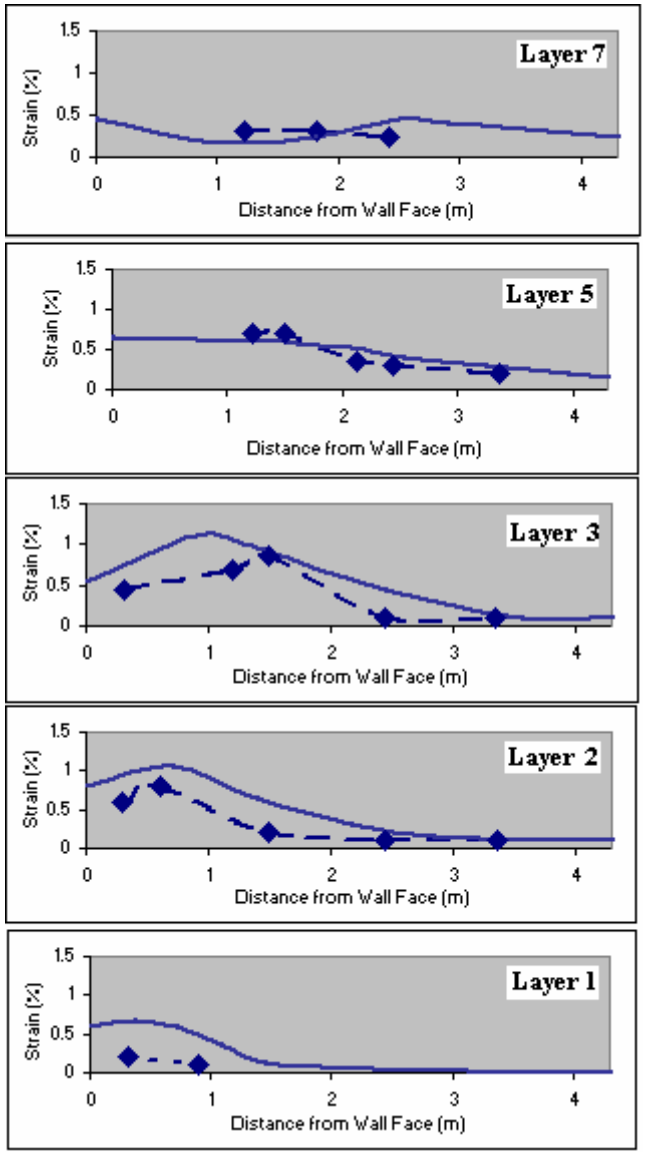

Fig. 5. Reinforcement strain distribution for Algonquin wall at the end of construction, solid line: results of analysis, dashed line: instrumentation measurements.

Reinforcement Load Distribution Factor

Fig. 6 shows the distribution of average reinforcement tensions (T_{ave}) that were obtained from results of model Algonquin versus the normalized height. The average reinforcement tensions were determined by multiplying the average predicted reinforcement strains with the reinforcement stiffness to represent the overall reinforcement tensions. Here

the reinforcement load distribution factor is defined by the ratio of T_{ave} in a reinforcement layer to the maximum average reinforcement load ($(T_{ave})_{max}$) in the wall. Fig. 6 indicates that the maximum value of T_{ave} is located at elevations between 0.6H to 0.25H.

The soil reinforcement load distribution factor can be determined using the K_0-stiffness method presented by Allen and Bathurst [2001] for geosynthetic reinforced walls as shown in Fig. 7. This new method was developed empirically through analysis of full-scale wall case histories. Not that this empirical distribution factor applies to walls constructed on a firm soil foundation. As shown in Fig. 7 there is a good agreement between the results of model and the K_0-stiffness method for the reinforcement load distribution factor.

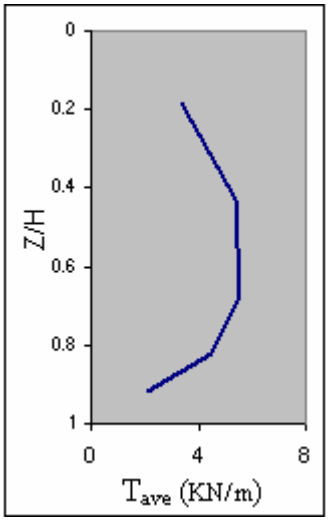

Fig. 6. Distribution of average reinforcement tensions at the end of construction.

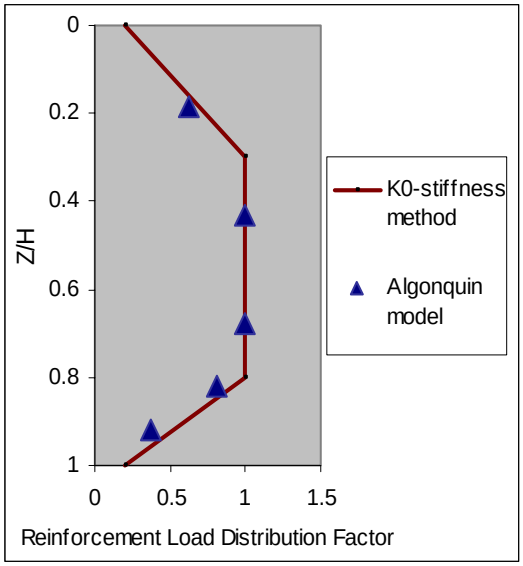

Fig. 7. Reinforcement load distribution factor.

Internal Vertical Stress and Axial Force of Facing Panels

Fig. 8 shows the vertical stress of model Algonquin wall at three elevations within the reinforced mass compared with γz values. Very small values of vertical stresses were considered just behind the facing panels, which further supported the concept of high vertical load transfer from the backfill to the panels. Away from the panels, good agreement exists between predicted and γz values. Fig. 9 shows that the axial force of facing panels is more than the weight of overlying facing panels (the weight of each facing panel is about 4 KN/m). It is attributed to shear stress on the back of the panels and vertical load transfer to the facing panels through the reinforcement connection clips. Less compaction effort was used for backfill placed just behind the panels, which likely increased fill settlement and load transfer to the panels.

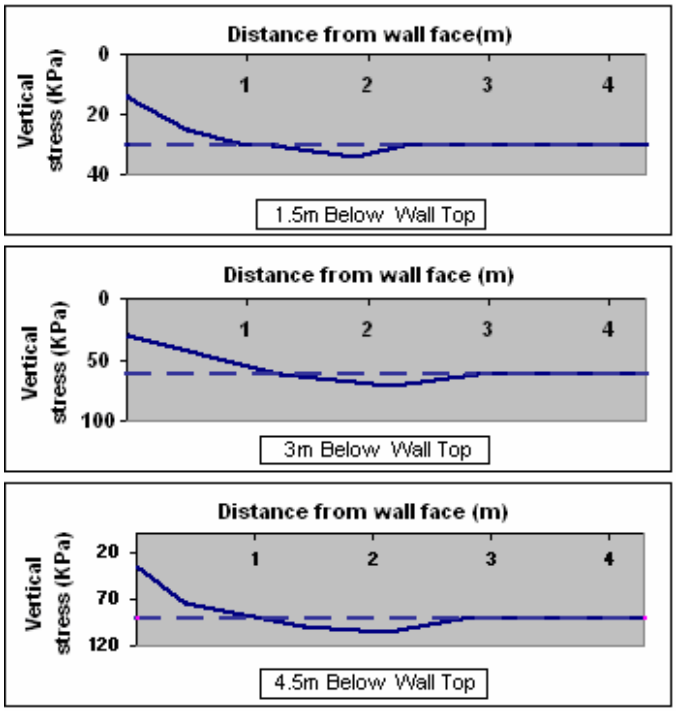

Fig. 8. Distribution of total vertical stress at three elevations within the reinforced soil at the end of construction, solid line: results of model, dashed line: γz values.

WALL PERFORMANCE DURING EARTHQUAKE

In the dynamic analysis a damping ratio of 10% is used. The dynamic damping is expressed by using α and β Rayleigh coefficients. These coefficients are proportional with stiffness and mass of the system.

Outward Lateral Displacement of Facing

Fig. 10 presents the calculated earthquake lateral displacement at 4 points along the height of the segmental facing. The figure indicates that the maximum lateral permanent deformation is

approximately 12cm and located near the crest of the segmental facing. It is noted that this out-of-alignment permanent deformation is approximately 2% of wall height and four times the value at the end of construction.

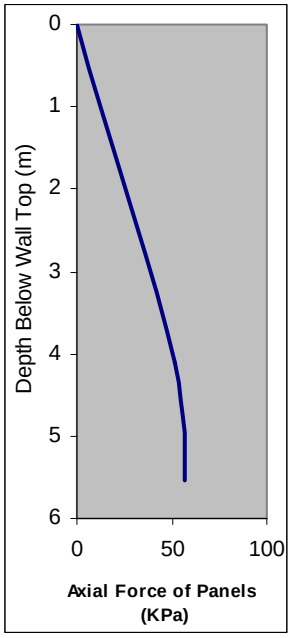

Fig. 9. Axial force of facing panels at the end of construction.

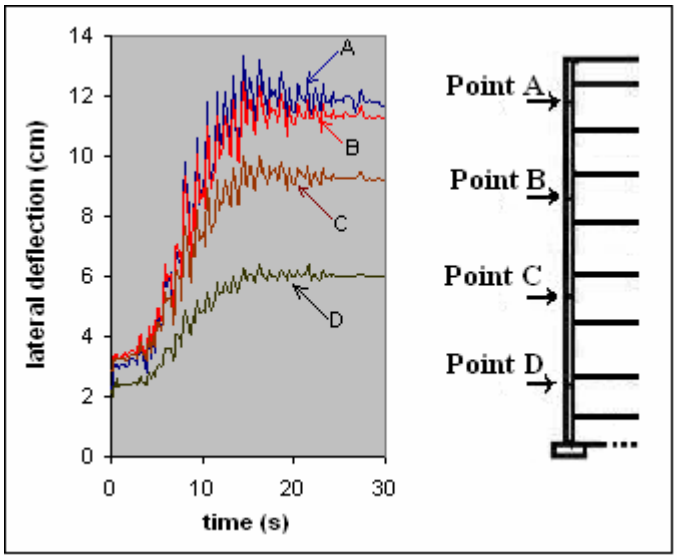

Fig. 10. Face deflection of Algonquin wall during earthquake.

Total (Dynamic) Axial Strain in Reinforcements

The distribution of total axial strain in the geogrid layers is shown in Fig. 11. From Fig. 11 it can be seen that the front end of the geogrid layers captured more load in comparison to the end of construction. Fig. 12 shows the maximum reinforcement strain in the geogrid layers. It is seen that a larger reinforcement strain was mobilized at the bottom of the wall, whereas the deformation was the largest at the top of the wall.

Authors suggest that the maximum dynamic strain in the geogrid layers can be reduced for the transient nature of the peak acceleration in the reinforced mass and the retained soils and the expectation that the inertial forces induced in the reinforced mass and the retained soil zone will not reach peak values at the same time during earthquake.

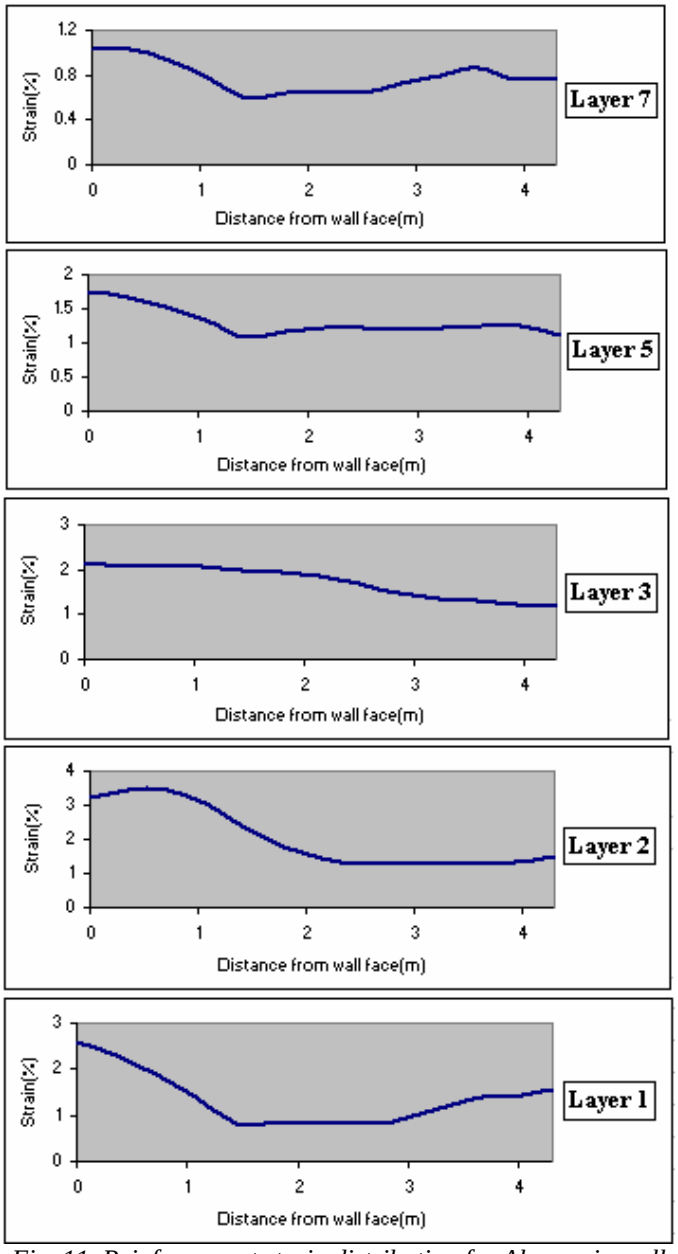

Fig. 11. Reinforcement strain distribution for Algonquin wall during earthquake.

Distribution of lateral earth pressure

Fig. 13 shows the calculated earthquake-included lateral earth pressures at four elevations within the reinforced mass which

were located at a distance of 1.0 m behind the back of facing panels. Fig. 14 shows the lateral permanent earth pressure normalized by γz ($\sigma_h/\gamma z$). It is seen that the permanent earth pressure was almost double the value at the end of construction, and the peak earth pressure ratio increased from a value of 0.2 to 0.42 under earthquake loading.

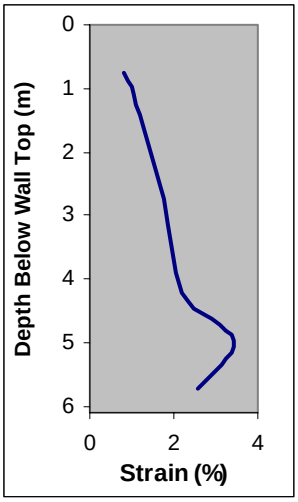

Fig. 12. Maximum reinforcement strain during earthquake.

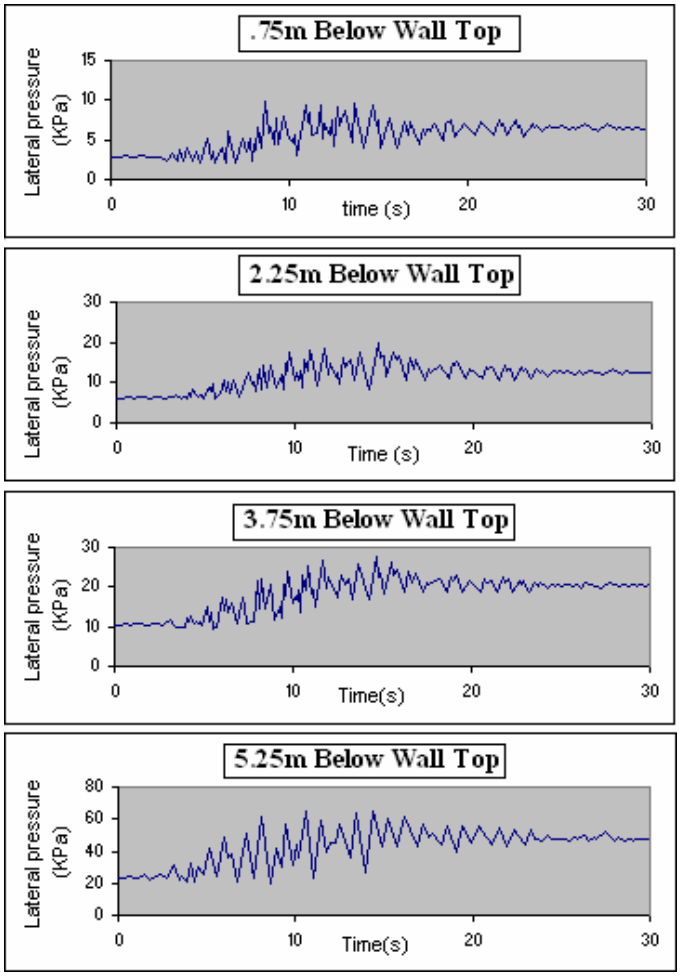

Fig. 13. *Distribution of lateral earth pressure* at four elevations *during earthquake.*

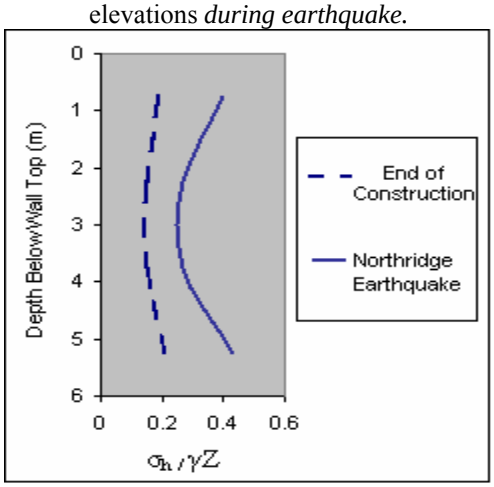

Fig. 14. lateral permanent earth pressure of wall.

CONCLUSIONS

This paper described a finite element analysis of a 6.1-m-high segmental retaining wall subjected to the Northridge earthquake was conducted using PLAXIS. The following conclusions were drawn based on the results of analysis:

End of Construction

1. The model was able to predict the field measurement of deflections and reinforced strain distribution of wall within reasonable ranges.
2. Small values of vertical stresses were considered just behind the facing panels, which further supported the concept of high vertical load transfer from the backfill to the panels.
3. Axial force of facing panels is more than the weight of overlaying facing panels. It is attributed to vertical stress transfer to the facing panels through the reinforcement connection clips.
4. There is a good agreement between the results of model and the K_0-stiffness method for the reinforcement load distribution factor.

Earthquake Loading

5. Analysis indicated that the out-of-alignment permanent deformation of the segmental wall was several times larger than that at the end of construction. The largest lateral displacement occurred at the top of the wall.
6. The strain in the reinforcement layers could be increased by 2 to 3 times comparing end of construction and earthquake loading conditions. The result indicated that a larger reinforcement strain was mobilized at the bottom of the wall, whereas the deformation was the largest at the top of the wall.

7. Earthquake loading resulted in an increase in the lateral earth pressure. The permanent earth pressure typically doubled the value at the end of construction.

REFERENCES

Allen, T.M. and R.J. Bathurst [2001]. "Prediction of Soil Reinforcement Loads in Mechanically Stabilized Earth (MSE) Walls at Working Stresses", Washington State Department of Transportation, Report WA-RD 522.1, 353 pp.

Bathurst, R.J. and K. Hatami [1998]. "Seismic Response Analysis of a Geosynthetic Reinforced Soil Retaining Wall", Geosynthetics Int., Vol. 5, Nos. 1-2, PP. 127-166.

Christopher, B.R. [1993]. "Deformation Response and Wall Stiffness in Relation to Reinforced Soil Wall Design", Ph.D. Dissertation, Purdue University, West Lafayette, Indiana, 354p.

Duncan, J.M., P. Byrne, K.S. Wong and p. Mabry [1980]. "Strength, Stress-Strain and Bulk Modulus Parameters Finite Element Analysis of Stress And Movement in Soil Masses", Report No. UCB/GT/80-1, Department of Civil Engineering, University of California, Berkeley, California, USA, 70 p.

Helwany, S.M.B., G. Reardon and J.T.H. Wu [1999]. "Effects of Backfill Type on the Performance of GRS Structures", Geotextiles and Geomembranes, J. Int. Geotextile Soc., 17(1), 1-16.

Helwany, S.M.B. and D. McCallen [2001]. "Seismic Analysis of Segmental Retaining Walls. II: Effects of Facing Details", J. Geotech.and Geoenvir. Engrg., ASCE, Vol. 127, No. 9, PP. 750-756.

Karpurapu, R. and R.J. Bathurst [1995]. "Behavior of Geosynthetic Reinforced Soil Retaining Walls Using the Finite Element Method", Comp. and Geotechnics , Vol. 17, No. 3, PP. 279-299.

Lee, W.F., R.D., Holtz and T.M. Allen [1999]. "Full Scale Geosynthetic Reinforced Retaining Walls: A Numerical Parametric Study", Proceeding of Geosynthetics'99, Boston, Vol. 2, PP. 935-948.

Rowe, R.K. and S. K. Ho [1992]. "A Review of The Behavior of Reinforced Soil Walls", Proc., Int. Symp. on Earth Reinforced Pract., IS-Kyushu '92, Earth Reinforcement Pract., H. Ochiai, N. Yasufuku, and K. Omine, eds., Balkema, Rotterdam, The Netherlands, 801-830.

Sandri, D. [1994]. "Retaining Wall Stand up to The Northridge Earthquake", Geotech. Fabrics Rep., Vol. 12, No. 4, PP. 30-31.

Element Analysis", Proc., Int. Geotechnical Symp. on Theory and pract. of Earth Reinforcement, IS-Kyushu ' Theory and

Segrestin, P. and M. J. Bastick [1988]. "Seismic Design of Reinforced Earth Retaining Wall - The Contribution of Finite Pract. of Earth Reinforcement, T. Yamanouchi, N. Miura, and H. Ochiai, eds., Balkema, Rotterdam, The Netherlands, 577-582.